NeuroImage 167 (2018) 354–365

Contents lists available at ScienceDirect

NeuroImage

journal homepage: www.elsevier.com/locate/neuroimage

Resting-state functional connectivity remains unaffected by preceding exposure to aversive visual stimuli

Léonie Geissmann [a,b,*], Leo Gschwind [a,b,c], Nathalie Schicktanz [a,b], Gunnar Deuring [d], Timm Rosburg [d], Kyrill Schwegler [a,b,e], Christiane Gerhards [a,b], Annette Milnik [b,c,e], Marlon O. Pflueger [d], Ralph Mager [d], Dominique J.F. de Quervain [a,b,e], David Coynel [a,b]

[a] Division of Cognitive Neuroscience, Department of Psychology, University of Basel, Birmannsgasse 8, 4055 Basel, Switzerland
[b] Transfaculty Research Platform Molecular and Cognitive Neurosciences (MCN), University of Basel, Birmannsgasse 8, 4055 Basel, Switzerland
[c] Division of Molecular Neuroscience, Department of Psychology, University of Basel, Birmannsgasse 8, 4055 Basel, Switzerland
[d] Department of Forensic Psychiatry, University Psychiatric Clinics Basel, Wilhelm Klein-Strasse 27, 4002 Basel, Switzerland
[e] Psychiatric University Clinics, University of Basel, 4055 Basel, Switzerland

ARTICLE INFO

Keywords:
Resting-state
Functional connectivity
fMRI
Amygdala
Emotion
Resting-state networks

ABSTRACT

While much is known about immediate brain activity changes induced by the confrontation with emotional stimuli, the subsequent temporal unfolding of emotions has yet to be explored. To investigate whether exposure to emotionally aversive pictures affects subsequent resting-state networks differently from exposure to neutral pictures, a resting-state fMRI study implementing a two-group repeated-measures design in healthy young adults ($N = 34$) was conducted. We focused on investigating (i) patterns of amygdala whole-brain and hippocampus connectivity in both a seed-to-voxel and seed-to-seed approach, (ii) whole-brain resting-state networks with an independent component analysis coupled with dual regression, and (iii) the amygdala's fractional amplitude of low frequency fluctuations, all while EEG recording potential fluctuations in vigilance. In spite of the successful emotion induction, as demonstrated by stimuli rating and a memory-facilitating effect of negative emotionality, none of the resting-state measures was differentially affected by picture valence. In conclusion, resting-state networks connectivity as well as the amygdala's low frequency oscillations appear to be unaffected by preceding exposure to widely used emotionally aversive visual stimuli in healthy young adults.

Introduction

Emotions are closely tied to cognitive, attentional and motivational processes. The amygdala strongly reacts to emotional stimuli and there is ample evidence that functional interactions of the amygdala with other brain regions are critically implicated in emotion processing upon acute emotional stimuli (Banks et al., 2007; Eippert et al., 2007; Erk et al., 2010; Townsend et al., 2013). The amygdala receives input from all sensory systems and polymodal cortices. Behavioral responses are generated primarily through amygdala projections to hypothalamic and brainstem centers involved in autonomic control. Among these is the locus coeruleus (LC), a major norepinephrine synthesis site. Norepinephrine pathways are important in maintaining arousal and level-setting for gathering sensory information and storing emotional memories (Venkatraman et al., 2017). Connections between the amygdala and the hippocampal complex contribute to the memory-enhancing effect of emotional arousal (Fastenrath et al., 2014; Richardson et al., 2004; Roozendaal et al., 2009), while the prefrontal cortex (PFC) plays a role in cognitively and emotionally interpreting affectively valenced stimuli, and in controlling the subsequent behavioral responses (Höistad and Barbas, 2008). In humans, top-down and bottom-up mechanisms orchestrated by interactions between the amygdala and medial PFC have been discussed extensively in the context of anxiety and emotion regulation (Kim et al., 2011).

Whereas much is known about the immediate effects of emotions on brain activations measured with blood-oxygen-level dependent contrast (BOLD) functional imaging during the acute emotional state (Murty et al., 2010; Verduyn et al., 2015; Waugh and Schirillo, 2012), little is known about the further temporal unfolding of emotions and their long-term neural consequences. On the behavioral level, there is ample evidence for such long-term consequences. For example, pathological anxiety may be expressed in excessive apprehension subsequent to immediate

* Corresponding author. Division of Cognitive Neuroscience, Department of Psychology, University of Basel, Birmannsgasse 8, 4055 Basel, Switzerland.
E-mail address: leonie.geissmann@unibas.ch (L. Geissmann).

https://doi.org/10.1016/j.neuroimage.2017.11.046
Received 2 June 2017; Accepted 21 November 2017
Available online 22 November 2017

emotion processing (Calhoon and Tye, 2015). Moreover, in animals it has been shown that the amygdala plays a key role in enhancing memory consolidation processes and, thereby, long-term memory of emotionally arousing information (Phelps and LeDoux, 2005; Roozendaal et al., 2009).

One possibility to investigate delayed neural consequences of emotional stimuli is to analyze functional connectivity (FC) in a resting-state period after an emotional task. The resting-state is defined as a state of nonattendance in an active task and absence of external stimulation (Barkhof et al., 2014), while FC reflects the temporal dependence of neural activity patterns of separated brain regions (van den Heuvel et al., 2010). The repertoire of functional networks utilized by the brain in action may persist in the resting-state, where they can be mapped as overlapping resting-state networks (RSN) (Biswal et al., 2010; Damoiseaux et al., 2006; Laird et al., 2011; Smith et al., 2009) using resting-state functional magnetic resonance imaging (rs-fMRI). Among the most commonly used approaches for identifying functionally interacting brain regions from rs-fMRI data are independent component analysis (ICA), seed-to-voxel, and seed-to-seed approaches (Smith et al., 2014; Whitfield-Gabrieli and Nieto-Castanon, 2012). Besides network measures, BOLD signal changes in regional spontaneous activity are valuable complements for characterizing resting-state low frequency oscillations (LFO), e.g. fractional amplitude of low frequency fluctuations (fALFF) (Zou et al., 2008).

Whereas initial cognitive theories have regarded the resting-state as a "default state of mind", it is becoming clearer now that cognitive activity also affects later rs-FC. Studies in healthy subjects have already indicated that the time following acute stressors is characterized by particular patterns of amygdala-FC, e.g. increased amygdala-FC after watching highly aversive video clips (van Marle et al., 2010). More precisely, female subjects not used to violent media watched a movie of 1.5 min duration while inside the MRI scanner. Directly afterwards, enhanced amygdala-FC with a set of predefined regions was observed (van Marle et al., 2010). Among those was the dorsal anterior cingulate cortex (dorsal ACC) and anterior insula (AI), which are implicated in the subjective experience of emotion, and the LC, which contributes to arousal by noradrenergic innervations to the amygdala. In another study, as much as 1 h after a well-established psychosocial stress task, increased amygdala-FC with cortical midline structures, pertaining to the default mode network (DMN), and the medial PFC was found (Veer et al., 2011). The authors discuss the increased amygdala-FC with DMN regions as reflecting stress-induced facilitation of self-evaluative processes under emotionally salient experiences. The enhancements in amygdala-medial PFC coupling may be an indicator of top-down processes (Kim et al., 2011; Veer et al., 2011).

Here we investigated if emotionally arousing pictures similar to stressful events can also induce changes in rs-FC. We chose a picture task because such tasks are widely used in human brain activation studies, and because viewing emotional pictures acutely increases activation in several brain regions, including the amygdala and hippocampus (Fastenrath et al., 2014; Murty et al., 2010; Rasch et al., 2009). Since emotional arousal is known to enhance not only memory encoding but also memory consolidation processes (Roozendaal et al., 2009), we hypothesized that such long-term effects may be reflected in increased amygdala rs-FC with brain regions like the hippocampus.

Implementing a repeated-measures mixed design with two experimental groups of equal size (total $N = 34$), a neutral-picture and a negative-picture group, we focused on the between-groups comparison in terms of changes in rs-FC from baseline (pre-intervention) to post-intervention (time point*group interaction). In a first step, we investigated FC of the amygdala with the whole brain in a seed-to-voxel approach, as well as with the hippocampus only in a ROI-to-ROI analysis. In a second step, we used ICA coupled with dual regression to assess functional connectivity changes in the brain in a more explorative way to address the diversity of networks potentially involved in emotion regulation. To get a complementary view on the amygdala's regional resting-state activity, we additionally extracted its mean fALFF. For validation purposes, the seed-based analyses done with amygdala masks were conducted with two segmentation procedures. Upon a more explorative background, we secondarily investigated FC of the hippocampus with the whole brain. Due to the uncontrolled nature of vigilance in rs-fMRI (Tagliazucchi and Laufs, 2014), we utilized simultaneous electroencephalography (EEG)-fMRI recordings to take into account in a post-hoc manner potential fluctuations in vigilance.

Materials and methods

Subjects

Thirty-four healthy, normal-weight (BMI 19 to 25) subjects aged 18 to 25 participated in this study ($M = 22.5$, $SD = 2.06$, range = 18.4 to 25.8). Male ($N_{male} = 14$) and female ($N_{female} = 20$) subjects did not significantly differ in age ($t(31.3) = 0.94$, $p = 0.35$). Participation was not possible if one or more of the following applied: regular intake of medical drugs with the exception of oral contraceptives, currently pregnant or breast-feeding, known or suspected non-compliance, drug or alcohol abuse, inability to follow the procedures of the study (e.g. due to language problems), present diagnosis of acute or chronic mental and/or somatic disorder, presently doing psychotherapy, not fulfilling MRI eligibility criteria. Previous participation in another study of the Transfaculty Research Platform Molecular and Cognitive Neurosciences (MCN), University of Basel, Switzerland (<2 years ago), if concordant visual stimuli employed, was also an exclusion criterion. For eligibility clarification, a psychologist screened subjects by telephone. When in doubt, assertion was obtained through medical counseling. Written informed consent was given at the study visit day. The study was conducted in approval with the local Ethics Committee, Ethikkommission Nordwest-und Zentralschweiz (EKNZ), Switzerland. The study took place between March and June 2015.

The method of allocating participants to a picture valence group (negative-group vs. neutral-group) was quasi-random: there was an alternation per participant in the order they were included in the study. Indispensably, towards the end of the study, three exceptions had to be made in order to equalize the ratio of experimental group within the factor sex. Subjects were instructed to refrain from caffeine intake and cigarette smoking at least 2 h, cannabis intake at least 2 weeks, alcohol and medical drug intake at least 24 h prior to commencement of the experiment, and to adhere to their personal sleeping habits the night before the examination.

Depression scores were measured with a screening questionnaire, the long version of the Allgemeine Depressionsskala (ADS) (Hautzinger and Bailer, 1993) (supplementary Table A1). Generally, there were no scores indicative for presence of depression (Table 1). However, two female subjects and one male subject met or surpassed the clinical threshold of 23 points. As exclusion of these subjects did not alter the results of the main brain imaging analyses (section "Seed-to-voxel and seed-to-seed analysis with bivariate correlation"), we retained them in the analyses while controlling for depression score by including it as a covariate (section "Brain imaging analysis").

Experimental procedure

The experimental procedure is illustrated in Fig. 1. Upon arrival, written informed consent was acquired and the participant was made familiar with the MRI environment. After this, about 50 min were spent filling out questionnaires while the investigator was attaching the EEG electrodes. Participants wore the EEG cap during the entire experiment. EEG was recorded in five sessions: shortly before the first MRI as a brief quality check, during both MRI sessions, during the pictorial rating task and throughout the free recall task. After satisfactory quality check of the EEG signal (impedances well below 20 kΩ; for reference and ground electrodes below 10 kΩ), the first MRI session followed, which took

Table 1
Descriptive statistics for demographical data and the measures of the three behavioral domains. Numbers represent the mean (*M*) and standard deviation (*SD*) of the negative- and neutral-groups individually. Between-group inferential statistics were obtained with Welch's two-sided *t*-tests for independent samples and denoted in *t*-statistic (*t*) and degrees of freedom (*df*). Sex counts are given in absolute numbers. For detailed description of the questionnaires please refer to Supplementary Table A1. Note some minor deviations from the number of subjects: for the NEO-subscales and the STAI state 1, data for two subjects was not available. There was missing data in the ESS for one subject. Two subjects were excluded from statistical tests involving RVDLT-recall performance. Numbers in bold indicate nominally significant *p*-values.

	Measure	Negative-group	Neutral-group	*t(df)*	*p*-value
		M(SD) ($N = 17$)	*M(SD)* ($N = 17$)		
Demographical data	Female	10	10		
	Male	7	7		
	Age	22.5(1.97)	22.6(2.20)	0.040(31.6)	
Pictorial rating task	IAPS arousal	11.4(12.4)	−5.09(9.40)	−4.36(29.8)	**<0.001**
	IAPS valence	−22.7(9.27)	7.25(10.7)	8.72(31.4)	**<0.0001**
	RVDLT size	16.7(12.2)	20.2 (17.0)	0.691(29.0)	0.495
	RVDLT form	−0.875(10.2)	7.05(16.0)	1.73(27.1)	0.096
Free recall task	IAPS correctly recalled	13.1(3.09)	10.5 (3.68)	−2.17(31.1)	**0.038**
	RVDLT correctly recalled	3.12(1.45)	3.00(1.41)	−0.25(30.0)	0.807
Questionnaires	NEO-neuroticism	16.0(6.48)	17.1 (4.83)	0.568(29.5)	0.575
	NEO-extraversion	31.8(6.02)	30.1(5.93)	−0.846(30.9)	0.404
	NEO-openness	29.2(6.40)	31.6 (6.67)	1.07(30.7)	0.291
	NEO-agreeableness	32.9(5.94)	33.9(5.02)	0.514(29.2)	0.611
	NEO-conscientiousness	31.9(7.35)	30.9(6.06)	−0.420(29)	0.678
	AIM-positive intensity	23.5(3.74)	26.7 (5.91)	1.91(27.1)	0.067
	AIM-negative intensity	19.9(7.29)	24.3(6.43)	1.87(31.5)	0.071
	AIM-serenity	18.8(5.29)	22.0(4.12)	1.99(30.2)	0.056
	STAI trait	35.7(6.76)	35.8 (6.49)	0.052(32.0)	0.959
	STAI state 1	29.5(9.27)	29.4 (4.76)	−0.021(20.3)	0.984
	STAI state 2	33.4(5.30)	30.5 (7.51)	−1.29(28.8)	0.206
	ADS-L	10.4(7.61)	11.2(6.63)	0.313(31.4)	0.757
	ESS	10.8(2.59)	8.81(2.97)	−2.01(29.8)	0.054

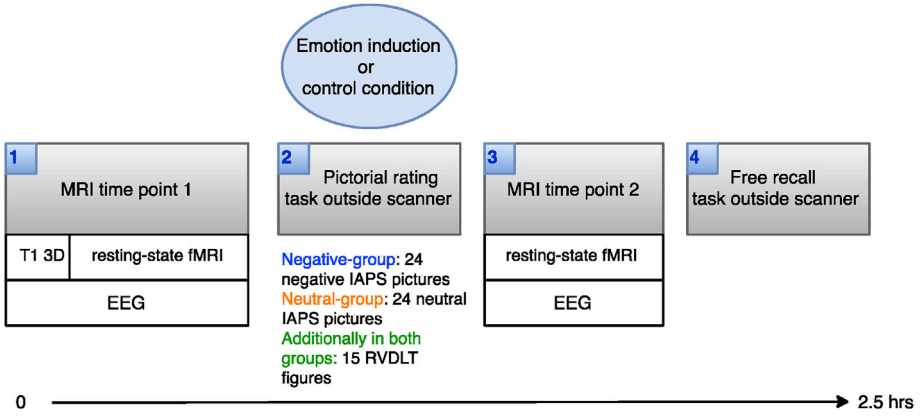

Fig. 1. Illustration of the experimental procedure. Not depicted in this figure are the questionnaires that were completed before and after the first MRI, as well as three of the total of five EEG recordings.

about 20 min. This started with the structural imaging. In between the first and second MRI sessions, subjects accomplished the pictorial rating task, which served as the emotion induction intervention, outside the MRI-scanner, for about 10 min. Information about stimuli valence was kept from the subjects until the pictorial rating task. From the study descriptions, subjects were aware that they might view emotionally aversive stimuli. Subsequent to the second rs-fMRI measurement, which lasted about 10 min, there was an unannounced free recall task, followed by follow-up questionnaires. Participation compensation was CHF 60.-. The study visit took approximately 2.5 h.

Behavioral measures

Pictorial rating task

The software Presentation® (Neurobehavioral Systems, Inc., Berkeley, CA, www.neurobs.com) was used for the pictorial rating task. Stimuli consisted of a total of 53 pictures selected from the International Affective Picture System (IAPS; Lang et al., 2005) and 16 geometrical figures taken from the Rey Visual Design Learning Task (RVDLT) (Spreen and Strauss, 1991). On the basis of normative valence and arousal scores of an American sample, pictures were assigned either to an emotionally neutral or emotionally negative category (supplementary Table A2). For the training session (see below), we exclusively used neutral pictures.

Depending on the experimental condition, for the main task either 24 neutral or 24 negative pictures were employed (neutral-group vs. negative-group) (supplementary Table A2). Negative emotional pictures were of various sorts, e.g., mutilated bodies, fearful faces, threatening animals, scenes depicting accidents and environmental pollution. Each of the 24 negative pictures matched one of the 24 neutral pictures corresponding to the following criteria: species (e.g., human, ungulate), perspective (scenery, single object, portrait), color spectrum, and number of individuals shown (e.g. portraits with neutral facial expression matched to a seriously injured face).

In addition to the emotional pictures (negative or neutral IAPS-pictures), the pictorial rating task included 16 geometrical figures (the same were used in both study groups) chosen from the RVDLT-set (Spreen and Strauss, 1991) and presented on a colored scrambled background we created using Adobe Photoshop CS3 (©2007 Adobe Systems Incorporated). It was composed of the task IAPS-images positioned next to one another, edited with a distortion and crystal filter in

such a way that the motives were no longer perceivable.

Participants were instructed to subjectively and intuitively rate the emotional pictures for valence (negative/positive) and arousal (calm/arousing), and the geometrical figures for form (height/width) and size (big/small) on a dimensional scale. The task was performed on a computer screen located at eye height about 40 cm away from the subject. Subjects submitted their ratings using a computer mouse on a visual-analog scale with a range of rating values ranging from -200 to +200. Each picture was presented for 2.5 s in a quasi-randomized order, with two pictures maximum in succession from any one category (IAPS-pictures vs. RVDLT-figures). The first and last two pictures presented were IAPS-pictures and the same for all individuals within their experimental group. Due to expected presentation order effects, these primacy and recency pictures were excluded from the analysis of the free recall and pictorial rating tasks. There was no time limit for rating.

To ensure clarity of the instructions, the task was preceded by a training session, in which five neutral IAPS-pictures and one RVDLT-figure were used. The task itself comprised 24 IAPS-pictures and 15 geometrical figures. All geometrical figures, as well as the IAPS-pictures of the training session, were the same for all subjects.

Free recall task

In a memory task after the second rs-fMRI, participants were given 10 min to freely recall as many photographs and geometrical figures as possible. They were instructed to describe briefly and precisely the remembered photographs in writing on the computer and to draw the geometrical figures on a blank paper. After 10 min had passed, participants were given the option of prolonging the time provided by 5 min, and then again by 5 min. The descriptions were rated for recall success independently by three trained investigators, the third of which then took a final decision about the score. Scores were calculated by summing the correctly remembered items, individually for photographs and figures, respectively. Due to misunderstanding of the instructions for the figure recall task two subjects were excluded from statistical analyses involving RVDLT-recall performance but included in all other analyses.

Questionnaires

A battery of self-report questionnaires in German language was used, including the long version of the Allgemeine Depressionsskala (Hautzinger and Bailer, 1993) for assessment of depression scores, the German version of the Affect intensity measure (Larsen and Diener, 1987) that assesses the intensity of a person's affective experiencing, the Edinburgh Handedness Inventory for evaluation of handedness (Oldfield, 1971), the Epworth Sleepiness Scale (Johns, 1991) for chance of dozing, and the NEO-FFI (Borkenau and Ostendorf, 1993) as a measure of personality dimensions. In order to measure anxiety levels the STAI state and trait versions (Laux et al., 1981) were used (supplementary Table A1). Additionally, a brief in-house questionnaire was filled in to check for adherence to study rules and to get some complementary information (e.g., thoughts during MRI, previous MRI examinations).

Brain imaging acquisition

All functional and structural MR images were acquired with a General Electric Discovery MR750w 3.0 T MRI scanner (General Electric Company, Milwaukee, USA) at bilddiagnostik.ch (Basel, Switzerland), equipped with a GE-28-elements GEM head and neck unit (General Electric Company, USA). The first MRI session started with the structural imaging (T1-weighted) and was directly followed by the first rs-fMRI acquisition (2D gradient-echo T2*-weighted echo-planar images). The second MRI session took place about 15 min after the end of the first MRI session, comprising an identical rs-fMRI sequence. In order to reduce head motion and dampen scanner noise, the subject was outfitted with ear protection and air cushions at each side of the head. For structural analysis, a T1 high-resolution anatomical sequence, 3D BRAVO (brain volume imaging), was performed, established with an oblique plane in an interleaved manner with the following scan parameters: 256 × 256 matrix, flip angle = 15°, field of view (FOV) = 250 mm and a bandwidth of 31.25, repetition time (TR) = 8.5 ms, echo time (TE) = 3 ms. To cover the entire brain, 164 slices, 1 mm thick, were implemented, leading to an in-plane resolution of 1 mm in all three directions. An inversion preparation pulse with a preparation time of 450 ms was also applied to increase T1-weighting.

Shortly before starting the rs-fMRI sequence, subjects were instructed to keep their eyes closed, to let their mind wander, not to fall asleep, and to move as little as possible. Functional images were acquired in an interleaved slice-order along the anterior commissure–posterior commissure with a single-shot, gradient-recalled echo-planar imaging sequence (TR = 3000 ms, TE = 30 ms, flip angle = 90°), consisting of 37 axial slices (slice thickness = 4 mm, slice spacing = 0.4 mm, FOV = 240 mm, in-plane matrix = 96 × 96, in-plane resolution = 2.5 mm^2). Two hundred volumes were acquired per scan. Additionally, four dummy samples were acquired before the actual start of the experiment to allow magnetization to reach a steady state, for a total acquisition time of 10.2 min.

Brain imaging analysis

Preprocessing of anatomical brain imaging data

Anatomical images were segmented into gray matter (GM), white matter (WM), and cerebrospinal fluid (CSF) by using SPM12 (Statistical Parametric Mapping, Wellcome Trust Centre for Neuroimaging, London). A diffeomorphic non-linear registration algorithm (diffeomorphic anatomical registration through exponentiated lie algebra; DARTEL) (Ashburner, 2007) was used to spatially normalize the segmented images to an in-house template brain (Heck et al., 2014), based on a sample of 1000 healthy subjects aged 18 to 35 comparable to the current study sample. The resulting flow fields were combined with an affine spatial transformation to normalize the images to the MNI space in order to render the findings comparable to other studies. Subject-specific amygdala and hippocampus masks were created for each hemisphere separately through segmentation with FreeSurfer (v.5.3.0; http://surfer.nmr.mgh.harvard.edu/). The segmented ROIs were normalized to the MNI space by applying the previous normalization parameters, and mean functional time series of the amygdalae and hippocampi were then calculated by averaging across all voxels within each mask, respectively. To take into account potential divergences in amygdala segmentation between different methods (Morey et al., 2009), we complemented the amygdala's segmentation by using FSL's FIRST segmentation tool (v. 5.0.9) in a subject-specific manner (Patenaude et al., 2011). While subcortical segmentation in FIRST proceeds with Bayesian shape and appearance models, FreeSurfer assigns a neuroanatomical label to each voxel based on probabilistic information automatically estimated from a large training set of expert measurements (Fischl et al., 2002; Morey et al., 2009; Patenaude et al., 2011). Unless specified otherwise, amygdala segmentations obtained with FreeSurfer were used.

Preprocessing of functional brain imaging data

The preprocessing pipeline prior to the analyses (sections "Seed-to-voxel and seed-to-seed analysis with bivariate correlation" to "Quality control of the independent components") included motion and slice-timing correction, normalization to the MNI space by using the transformation computed on the anatomical data, and smoothing with an 8 mm FWHM isotropic Gaussian Kernel. The experimental setup for all second-level analyses encompassed two second-level covariates of interest (negative- and neutral-group) and three of no interest (sex, age and depression score, all mean-centered), which were incorporated in consideration of their associations with measures of rs-FC (Andrews-Hanna et al., 2007; Fair et al., 2008; Ferreira and Busatto, 2013; Hjelmervik et al., 2014; Sheline et al., 2010). ART (Artifact Detection Tools; developed by Stanford Medicine, Center for Interdisciplinary Brain Sciences Research), an analysis software for detection of motion artifact

sources in fMRI time series, was implemented to provide movement regressor files as covariates in the first-level analyses. These are called "art_regression_outliers_and_movement.mat" per default and contain regressors to describe three translation, three rotation, one composite motion score and a variable number of outliers. Time points exceeding the movement threshold of 2 mm, or a *z*-value of 9 in the *z*-normalized global BOLD, were defined as outliers. Composite motion describes the maximal movement of any voxel within the brain bounding box in mm. For baseline and post-intervention resting-state, there were outliers in six and five subjects with maximum counts of 15 and 18 time points, respectively.

Seed-to-voxel and seed-to-seed analysis with bivariate correlation

For the seed-to-voxel approach, the functional connectivity toolbox Conn v.15c (www.nitrc.org/projects/conn) was used (Whitfield-Gabrieli and Nieto-Castanon, 2012). WM and CSF masks obtained from the segmentation of the anatomical images were coregistered to the functional space and considered subject- and session-specific noise regions of interest (ROI). Their respective time series were decomposed into 2 principal components by using a principal component analysis of the multivariate BOLD signal within each ROI with the CompCor method (Behzadi et al., 2007), and then regressed from the BOLD time series at each voxel. Such a flexible method is particularly appropriate for fMRI noise sources as cardiac and respiratory effects do not show a common spatial distribution across the brain (Behzadi et al., 2007). The temporal time series characterizing subject motion (three rotation and three translation parameters, and their first-order derivatives, i.e. ART motion parameters) were also removed from the BOLD data as temporal first-level covariates. The data were then band-pass filtered (0.01 Hz<f<0.1 Hz).

For main and secondary analyses, mean time series of the bilateral amygdala and bilateral hippocampus, respectively, were used as seed-ROI. There are two reasons for using the bilateral amygdala. First, previous studies investigating amygdala-FC (section "Introduction") used the bilateral amygdala as seed-ROI. Second, studies have shown robust effects in bilateral amygdala activation when viewing negative IAPS pictures (section "Discussion"). The first-level step comprised a whole-brain bivariate correlation analysis between the residual voxel-wise BOLD time series and the ROI time series. In case of amygdala-hippocampus ROI-to-ROI analysis, FC was defined as bivariate Pearson's correlation between mean time series of the respective ROI pair. Second-level analyses consisted of a linear model including the first-level estimates for both rs-fMRI sessions (within-subjects factor: time point), both groups (between-subjects factor: group), and their interaction. The main contrast of interest was the interaction time point*group. The threshold for significance was set at voxel-p-uncorrected < 0.001 and cluster-p-FWE-corrected < 0.05, as has been used previously (Chai et al., 2011; Chai et al., 2014; Manning et al., 2015).

Spatial decomposition into independent components and dual regression

FSL's MELODIC 3.0 (Jenkinson et al., 2012) uses independent component analysis (ICA) to decompose a single or multiple 4D datasets into different spatial and temporal components (http://fsl.fmrib.ox.ac.uk/fsl/fslwiki/MELODIC). We implemented MELODIC's spatial ICA to decompose the brain's low-frequency fluctuations at resting-session 1 for all 34 subjects. In consideration of our intention to pursue a data-driven, explorative approach, it has been recommended to include the whole set of ICs in subsequent tests for between-group differences (http://fsl.fmrib.ox.ac.uk/fslcourse/lectures/practicals/melodic/). Based on recent reports (Biswal et al., 2010), and in order to maintain a reasonable level of overview, we manually set the number of dimensions to be estimated with MELODIC to d = 20. Under the assumption that the 10 consistently reported networks (e.g., Biswal et al., 2010; Damoiseaux et al., 2006; Laird et al., 2011) will be subsumed to interpretable ICs in this solution, this allowed us to proceed with a pertinent quantity of ICs. Then, the set of spatial maps from the group-level analysis of the 20 dimensions solution was used to generate subject-specific versions of the spatial maps, and associated time series, using dual regression (Filippini et al., 2009). First, for each subject, the group-average set of spatial maps (from baseline resting-state) was regressed (as spatial regressors in multiple regression) into the subject's 4D space-time dataset from each rs-fMRI session. This resulted in a set of subject-specific time series, one per group-level spatial map (from baseline resting-state) for each rs-fMRI session. Next, those time series were regressed (as temporal regressors, again in multiple regression) into the same 4D dataset, resulting in a set of subject-specific maps, one per group-level spatial map for each subject. We predicted that one or more of the 20 spatial networks would underlie a different change from pre-intervention resting-state to post-intervention resting-state depending on the emotionality of the presented pictures. For each subject, we calculated the difference between session 2 and session 1 (i.e. subtracting session 2 from session 1). Those files were the input to FSL's randomise permutation-testing tool (Winkler et al., 2014) with 5000 permutations. The model comprised the mean-centered covariates of no interest sex, age, and depression score (ADS). The two contrasts of interest were (i) negative-group > neutral-group and (ii) neutral-group > negative-group. The p-FWE-voxel-corrected output files from FSL's randomise were further corrected for the amount of RSNs with the Bonferroni method.

Quality control of the independent components

MELODIC's decomposition will result in both functionally coherent RSNs as well as spatially structured artifacts (Smith et al., 2014) not necessarily represented by delimited components. An initial quality control of the 20 networks' spatial patterns was performed. The ICs' time courses, frequency spectra and spatial distributions were visually compared with previous reports (Damoiseaux et al., 2006; Smith et al., 2009). We further quantified the similarity of the networks to resting-state templates of 10 RSNs, available on http://www.fmrib.ox.ac.uk/datasets/brainmap+rsns/ (retrieved 07/07/16), described in Smith et al. (2009). These template networks circumscribe three visual networks (medial, occipital pole, lateral visual areas; 1-3), the default mode network (DMN) a cerebellum network (CN), the sensorimotor network (SMN), the auditory network (ADT), executive control network (ECN) and left/right fronto-parietal networks (LFPN, RFPN). These RSNs have been robustly detected in a number of independent studies (e.g., Biswal et al., 2010; Damoiseaux et al., 2006; Laird et al., 2011). We identified the template RSN that had the highest spatial correlation to our networks by using FSL's spatial cross-correlation, after binarizing the inputs at $z > |2|$.

Fractional amplitude of low frequency fluctuations

As a method to measure LFO, fALFF has recently been shown to be superior to the originally used ALFF due to its higher sensitivity and specificity of detecting spontaneous brain activity (Zou et al., 2008). Extraction of fALFF was performed by using the Data Processing Assistant for Resting-State fMRI (DPARSF, v. 4.1) (Chao-Gan and Yu-Feng, 2010), which is based on SPM and the toolbox for Data Processing & Analysis of Brain Imaging (DPABI). Specific preprocessing of structural and functional images was conducted in DPARSF. This included normalization with DARTEL for structural images, slice timing correction, realignment, smoothing, head motion correction with Friston 24 head motion parameters (Friston et al., 1996) and removal of WM and CSF signals for functional images. FSL's fslmeants was used to extract the mean of the time course of fALFF in rs-fMRI session 2 in the left and right amygdala, respectively, for each subject. These values were then subjected to group-level analyses of variance to test for time point*group interaction effects with the mean-centered covariates of no interest sex, age and depression score (ADS), as implemented in R (R Core Team., 2015).

Electroencephalography

EEG recording

The EEG recordings, conducted with a similar setting as Zotev et al.

(2014), were performed simultaneously with the rs-fMRI acquisitions by using the Brain Products' MR-compatible EEG system. Each subject wore an MR-compatible EEG cap (BrainCap MR from EASYCAP GmbH) throughout the experiment. The cap is fitted with 32 EEG electrodes (including the reference electrode), arranged according to the international 10-20 system, and one electrocardiographic (ECG) electrode placed on the subject's back. The EEG amplifier (BrainAmp MR plus from Brain Products GmbH) was positioned just outside the MRI scanner bore near the axis of the magnet. The electrical cable connecting the EEG cap to the amplifier was fixed in place by using a sandbag. The amplifier was connected to the PC interface outside the scanner room via fiber optic cable. The EEG system's clock was synchronized with the 10 MHz MRI-scanner's clock by using Brain Products' SyncBox device. The EEG signal acquisition was performed in BrainVision Recorder Professional (v. 1.20.0801) with 16-bit analog-to-digital conversion and 5000 Hz sampling rate, providing 0.2 ms temporal and 0.5 μV measurement resolution. The EEG signals were measured relative to FCz and filtered online between 0.016 Hz (10 s time constant) and 250 Hz (Zotev et al., 2014).

EEG preprocessing

All EEG data were processed in EEGLAB (v. 13.5.4b) running on Matlab R2014a (Mathworks). The large steady magnetic field B_0 and the fast time varying fields generated by the MR imaging sequence induce substantial artifacts in EEG data collected in an MRI-environment (Moosmann et al., 2009). Therefore, correction for gradient-related and ballistocardiographic (BCG) artifacts is required. We accomplished this correction with the Bergen plugin for EEGLAB (Allen et al., 2000; Moosmann et al., 2009). First, the fMRI volume onsets were detected via an autocorrelation method on the basis of an automatically selected channel premised on its median variance. This automatically detected channel was then manually checked and accepted. The threshold defining the occurrence of an fMRI gradient artifact was based on the first derivative (gradient value) of the EEG signal, specified in percentage relative to the maximum value of the gradient of the artifact signal. The artifact duration was defined as the time between the volume onset and the time point immediately before the subsequent volume onset marker (i.e. start = 0, end = TR; continuous recording). Next, baseline correction of the artifact periods defined in the previous step was done by using the mean of the artifact period itself. A realignment parameter-informed algorithm was used for correction for the gradient artifacts (Moosmann et al., 2009). This algorithm is based on an extension of template subtraction and performs particularly well in case of abrupt head movements. Following the fMRI gradient-artifact correction, the data was resampled to 500 Hz, QRS events were detected, and BCG artifacts removed with an artifact subtraction method, implemented in the FMRIB plug-in for EEGLAB, provided by the University of Oxford Centre for Functional MRI of the Brain (Iannetti et al., 2005; Niazy et al., 2005). Unsatisfactory cleaning of the gradient-related artifacts, as well as recording problems in one individual, led to valid EEG data for a total of 31 and 32 subjects for each rs-fMRI session, respectively.

Assessment of vigilance

Vigilance at different time points was dichotomously divided into relaxed wakefulness and drowsiness, henceforth referred to respectively as stage A and B, following an established procedure (Hegerl et al., 2008; Olbrich et al., 2009). This procedure retains much of a standard vigilance and sleep scoring (Rechtschaffen and Kales, 1968). Briefly put, this extended approach for vigilance scoring (Hegerl et al., 2008; Olbrich et al., 2009) centers on the concept of spatial redistribution of spectral alpha power and its diminishment during the transition from wakefulness to drowsiness. Building upon this, the procedure was as follows: for each subject and each resting-session, we split the whole rs-EEG according to the TR of the rs-fMRI sequence (3 s) leading to a total of 204 bins of 3 s duration (1500 EEG sampling points). Spectra for each bin were calculated with EEGLAB's spectopo-function, which uses Matlab's pwelch-function for obtaining Welch's power spectral density estimates. Bins were defined as an A-stage if at least one of channels O1, O2, F3, and F4 showed a higher power for the range 8–12 Hz than for 2 to 8 Hz; else, the bin was considered a B-stage. The former two electrodes correspond to the occipital, the latter two to the frontal parts of the brain.

Before vigilance staging, a first-level outlier correction was applied to the spectral power of the two frequency bands for each channel and each resting-session in two stages: (i) linear interpolation (R function approx from the stats-package), (ii) remaining outliers (i.e. those that could not be interpolated because they were either at the end or beginning of the sequence) were replaced by the respective channel's mean spectral power. Outliers were defined as time points below or above the tenth and ninetieth percentiles, respectively. Since the spectral estimations obtained from the Welch's method may take on negative values, those values were then log-transformed to positive values in order to form interpretable ratios.

Effect of vigilance fluctuations on the BOLD signal

With SPM12, we tested the extent to which the EEG-derived vigilance regressor was associated with the BOLD signal. First, the fully preprocessed images, i.e. after performing standard and resting-state-specific preprocessing using Conn, for each subject were used as input to estimate first-level contrast images with the HRF-convolved binary covariate vigilance stage (A = 0, B = 1) to test for voxels that would show a significantly (i) higher or (ii) lower activity change jointly with this regressor in a second-level analysis. Model parameters were estimated by using Restricted Maximum Likelihood specified with an autoregressive error model.

Statistical analysis of behavioral data

Analyses of behavioral data, unless specified otherwise, were performed in R Studio (R Core Team, 2015). For inferential statistics of behavioral data, the threshold of significance was set to $p < 0.05$. Between-group differences were tested for by means of two-sided Welch-*t*-tests for independent samples. Repeated-measures between-group differences and corresponding interactions were analyzed in mixed linear models with group as between-subjects factor and session as within-subjects factor, implemented in the R library nlme (v. 3.1–131). Non-directional associations of quantitative variables were tested for with pairwise-complete Pearson's correlation.

Results

Behavioral data

Pictorial rating task

As expected, subjects in the negative-group rated task IAPS pictures as less pleasurable and more arousing than did subjects in the neutral-group ($t(31.4) = 8.72$, $p < 0.001$ for valence; $t(29.8) = -4.36$, $p < 0.001$ for arousal). Size and form rating of geometrical figures did not significantly differ between the groups ($t(29) = 0.69$, $p = 0.49$; $t(27.1) = 1.73$, $p = 0.1$) (Table 1).

Free recall task

In recalling task IAPS-pictures, subjects in the negative-group performed better than subjects in the neutral-group ($t(31.1) = -2.17$, $p = 0.04$), with an average of 10.5 freely recalled task IAPS-pictures in the neutral-group ($SD_{neu} = 3.68$), and 13.1 in the negative-group ($SD_{neg} = 3.09$). In contrast, there were no between-group differences in the number of correctly recalled RVDLT-figures ($t(30) = -0.25$, $p = 0.81$) (Table 1), nor was there an association in recall performance between these two types of visual stimuli ($t(32) = -1.25$, $p = 0.22$, Pearson's $r = -0.216$).

Questionnaires

There were no significant group differences in NEO-FFI, AIM

subscales, or in STAI trait anxiety (Table 1). With regard to state anxiety (STAI state), there was no significant time point*group interaction ($F(1,30) = 0.91$, $p = 0.35$), and no main effect of group or session ($F(1,31) = 2.88$, $p = 0.42$; $F(1,32) = 0.68$, $p = 0.42$).

Resting-state fMRI

Seed-to-whole brain and seed-to-seed functional connectivity

Overall, baseline FC of the bilateral amygdala showed widespread connectivity clusters across the whole brain ($F_{min}(4,58) = 5.33$, minimum number of voxels in one cluster = 63), e.g. covering the temporal poles, precentral gyri, frontal orbital cortices, right middle frontal gyrus, insular cortices (Fig. 2a). There was no significant time point*group interaction. There was also no main effect of time point (group-invariant effect of the task, see Fig. 2b for amygdala-WB-FC at post-intervention), nor a main effect of any of the dimensional behavioral variables NEO-neuroticism, STAI trait anxiety, AIM affect reactivity, and ADS depression score. Post-hoc tests showed that the groups did not diverge in amygdala-FC either at the baseline or at the post-intervention rs-fMRI after the pictorial rating task. Furthermore, amygdala-hippocampus-FC did not reveal a significant time point*group interaction. All these results remained non-significant also if the right and left amygdala, and in case of the ROI-to-ROI analysis left and right hippocampus, served as separate seed-ROIs.

When using FIRST's instead of FreeSurfer's amygdala segmentations, there was still no time point*group interaction and no main effect of time point. While there was a main effect of segmentation method for baseline amygdala-FC ($F_{min}(2,29) = 8.85$, minimum number of voxels in one cluster = 56), including regions spanning temporal poles, subcallosal cortex, frontal orbital cortices, frontal medial cortex (supplementary Figure A1), the interaction time point*segmentation (mean of bilateral amygdala FIRST vs. FreeSurfer) was non-significant.

The bilateral hippocampus was extensively functionally connected to other brain regions at baseline ($F_{min}(4,58) = 5.33$, minimum number of voxels in one cluster = 51), e.g. frontal and temporal poles, lingual gyri, OFC, cingulate gyrus, thalamus, subcallosal cortex, insular cortex (Fig. 3a; Fig. 3b for post-intervention rs-fMRI). The same negative findings as for the amygdala apply to the hippocampus. Note that the hippocampus was segmented uniquely with FreeSurfer.

Spatial decomposition into independent components and dual regression

Upon visual inspection of the 20 ICs' time courses, frequency spectra and spatial distributions, we regarded some ICs as nuisance while others as reflecting actual brain activation, based on previous reports (Damoiseaux et al., 2006; Smith et al., 2009). The validity of the 20 networks (Fig. 4) was further investigated by comparing them to templates of 10 validated RSNs. The template networks VN1, VN3, CBN, ECN, and RFPN each were related to two networks, while each of the remaining five matched one (Table 2, supplementary Figure A2a-A2o). Testing the contrasts (i) negative-group > neutral-group, and (ii) neutral-group > negative-group showed that none of the 20 networks exhibited an emotionality-dependent change from resting-session 1 to resting-session 2 (even at nominal significance level, i.e. without correcting for the number of networks tested).

Fractional amplitude of low frequency fluctuations

There was no time point*group interaction in fALFF for either left ($F(1,32) = 0.28$, $p = 0.6$) or right ($F(1,32) = 1.15$, $p = 0.291$) amygdala (Fig. 5).

Motion outliers

There was no main effect in the amount of motion outliers (section "Preprocessing of functional brain imaging data") for the factors group ($F(1,32) = 0.492$, $p = 0.488$) and time point ($F(1,32) = 0.126$, $p = 0.725$), nor was there an interaction time point*group ($F(1,32) = 0.04$, $p = 0.842$).

Resting-state EEG

EEG data collection

To warrant our subjects the highest safety possible, in 15 subjects, the

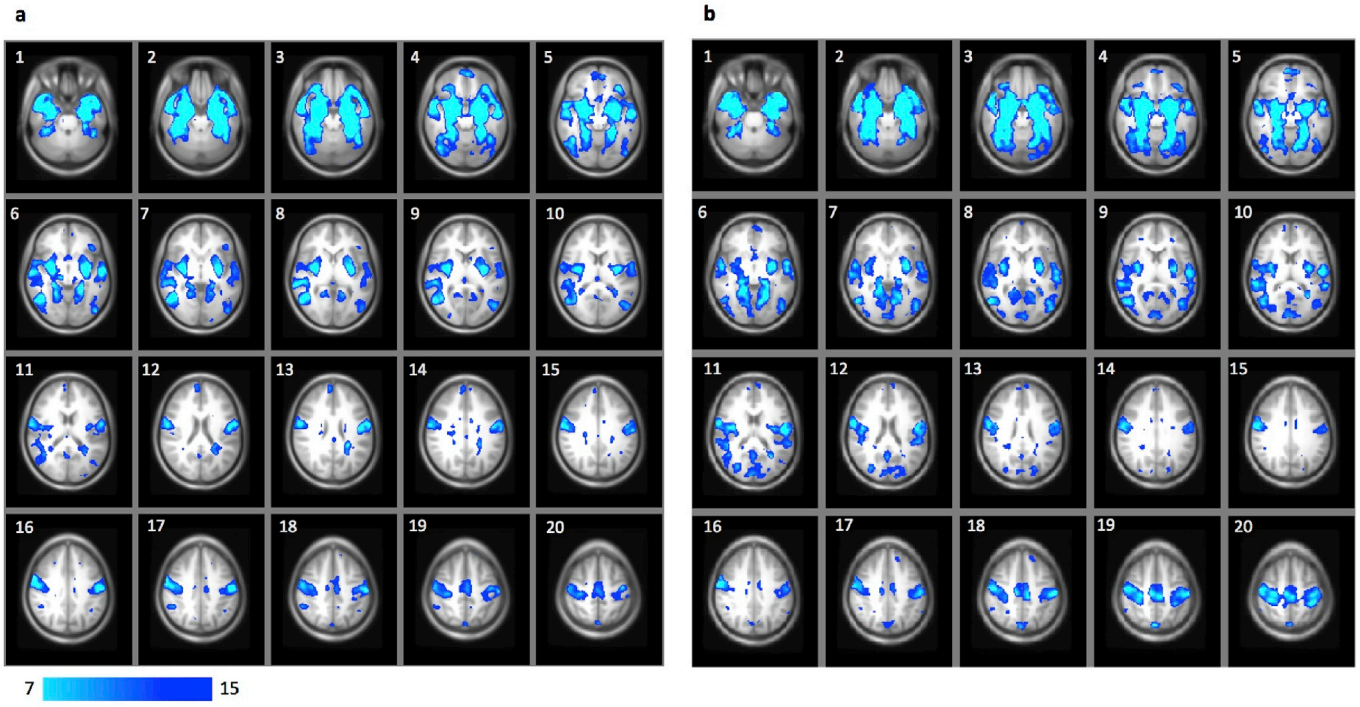

Fig. 2. Brain maps thresholded at $F > 7$ depicting amygdala-whole brain functional connectivity clusters across both groups **(a)** at baseline and **(b)** after the pictorial rating task (p-voxel-uncorrected < 0.001 and p-cluster-FWE-corrected < 0.05; $F_{min}(4,58) = 5.33$ for both sessions), depicted in axial slices (Z = 26.40 to Z = 57.20 in MNI space). Abbreviations: FWE = family-wise error rate; F=F-statistic.

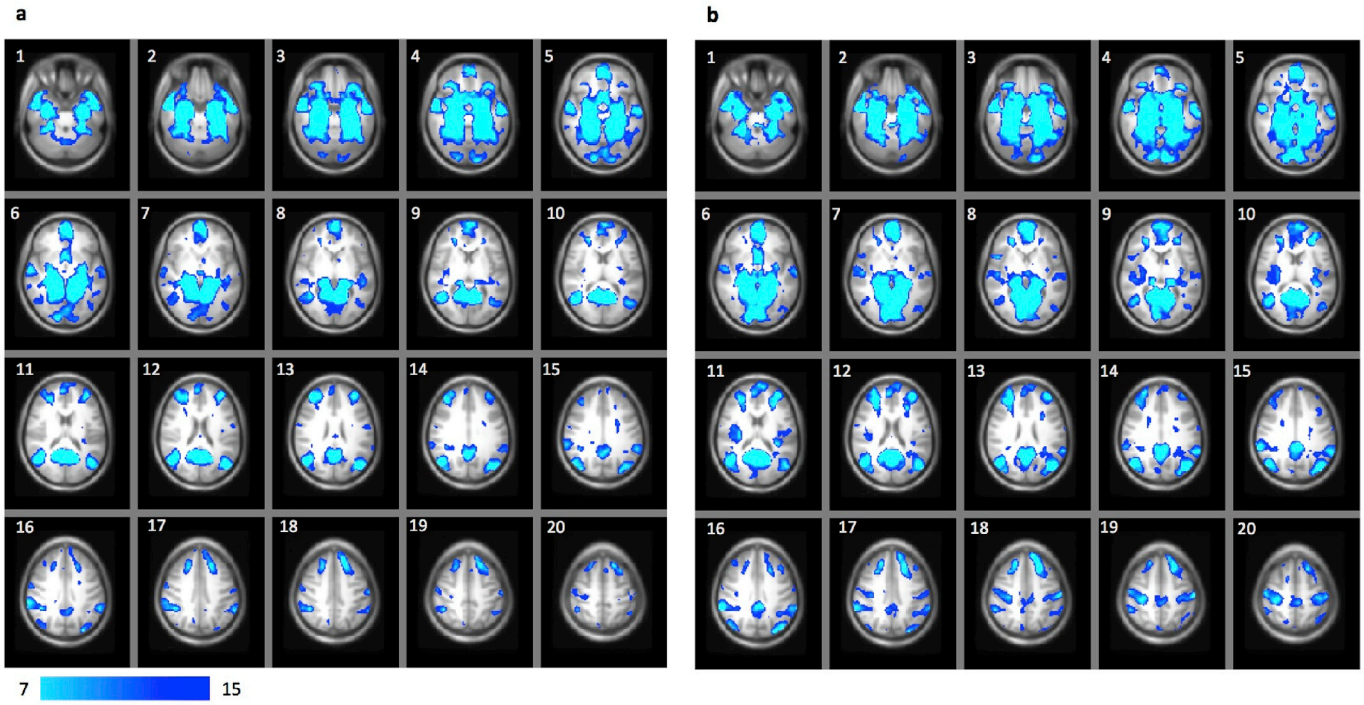

Fig. 3. Brain maps thresholded at $F > 7$ showing hippocampus-whole brain functional connectivity clusters across both groups **(a)** at baseline and **(b)** after the pictorial rating task (p-voxel-uncorrected < 0.001 and p-cluster-FWE-corrected < 0.05; $F_{min}(4,58) = 5.33$ for both sessions), depicted in axial slices (Z = 26.40 to Z = 57.20 in MNI space). Abbreviations: FWE = family-wise error rate; F=F-statistic.

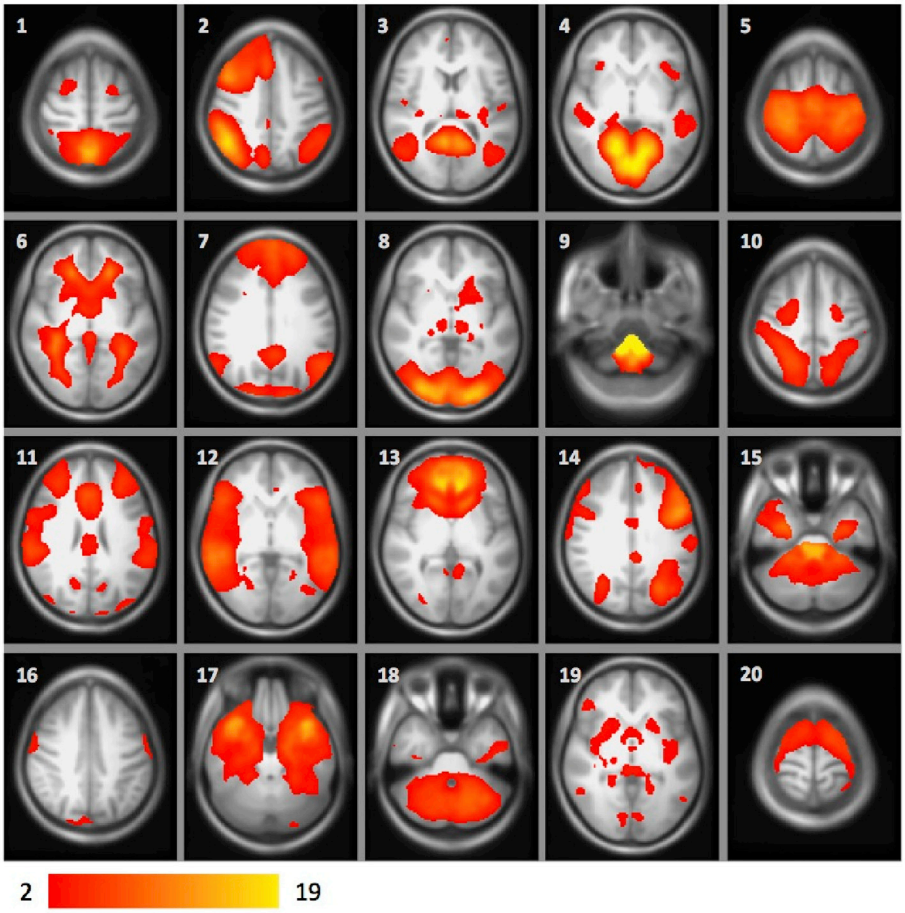

Fig. 4. Brain maps illustrating the 20 ICs as estimated with FSL's MELODIC for spatial decomposition of all subjects' 4D data sets of baseline resting-state functional connectivity. The enumeration of these ICs corresponds to the ones used in Table 2. Abbreviations: IC = independent component.

Table 2
Table demonstrating the spatial overlap of the independent components from resting-session 1 with 10 robust template resting-state networks, obtained with cross-correlation. Brain maps of these spatial overlaps can be found in supplementary Fig. A2a-2o (as indexed in the table). Abbreviations: VN = visual network; DMN = default mode network; CN = cerebellum network; SMN = sensorimotor network; ADT = auditory network; ECN = executive control network; LFPN = left frontoparietal network; RFPN = right frontoparietal network.

Template network	IC	*r*	Index
VN1	4	0.760	1a
VN1	8	0.222	1b
VN2	8	0.701	1c
VN3	10	0.398	1d
VN3	12	0.387	1e
DMN	3	0.445	1f
CN	15	0.238	1g
CN	18	0.672	1h
SMN	5	0.681	1i
ADT	12	0.472	1j
ECN	2	0.245	1k
ECN	7	0.318	1l
LFPN	2	0.349	1m
LFPN	11	0.490	1n
RFPN	14	0.633	1o

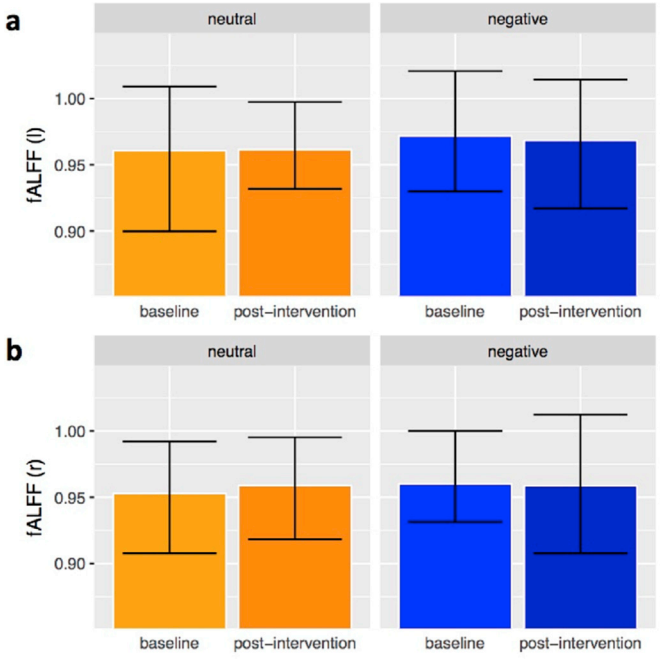

Fig. 5. Bar charts showing baseline and post-intervention fALFF values of the left **(a)** and right **(b)** amygdala for each group separately. Error bars depict standard error of the mean. Abbreviations: fALFF = fractional amplitude of low frequency fluctuations; l = left; r = right.

EEG electrodes had to be mended in between the MRI sessions due to poor electrode impedances. This was the case for four, eight, and five subjects before the first rs-fMRI, after the first rs-fMRI, and after the pictorial rating task, respectively. This prolonged the experiment by about 3 min for the subjects concerned.

Frequency of vigilance stage A and B

As described in section "Assessment of vigilance", vigilance was classified into the two discrete stages wakefulness and drowsiness (stages A and B, respectively) (Hegerl et al., 2008; Olbrich et al., 2009). For resting-session 1, the majority of participants showed a higher proportion of A-stages than B-stages for the total of that resting-session ($M = 0.70$, $SD = 0.29$, range = 0.15 to 0.99). This tendency remained approximately the same at resting-session 2 ($M = 0.76$, $SD = 0.26$, range = 0.18 to 1). There was no time point*group interaction ($F(1,28) = 1.86$, $p = 0.18$). Of note, all subjects except for two stated having been awake at all times.

Effect of vigilance fluctuations on the BOLD signal

There was no significant effect of the binary first-level regressor vigilance at any voxel at *p*-FDR-corrected at neither resting-session 1 nor resting-session 2.

Discussion

We implemented a two-group repeated-measures rs-fMRI design to investigate functional networks and functional connectivity of the amygdala in healthy young adults. The present study aimed to reveal the brain states that characterize delayed emotion regulation following exposure to visual stimuli of negative compared to neutral valence. Overall, the amygdala showed widespread connectivity clusters across the whole brain, e.g. covering temporal poles, precentral gyrus, frontal orbital cortices, right middle frontal gyrus, and insular cortices, in line with previous findings from rs-fMRI in humans (Roy et al., 2009). This was applicable for both rs-fMRI sessions. Compliant with these findings, tracer studies in rhesus monkeys provide strong evidence for projections from specific orbitofrontal, medial prefrontal and temporal cortical pathways onto excitatory and inhibitory pathways in the amygdala, suggested to interact in emotion mechanisms (Ghashghaei and Barbas, 2002; Höistad and Barbas, 2008).

Whereas we expected to observe distinct bilateral amygdala-FC between-session changes in subjects who had viewed negative pictures, as compared to those who had viewed neutral pictures (time point*group interaction), there was no such effect, not even in amygdala-hippocampus FC. In the light of the plurality of cognitive processes in which the amygdala is involved (e.g., impulsivity, appetitive motivation) (Kerr et al., 2015; Passamonti et al., 2008; C. Xie et al., 2011) and the many brain regions implicated in affective processes, e.g., the cerebellum (Baumann and Mattingley, 2012; Riedel et al., 2015), and medial prefrontal regions (Phan et al., 2002), we intended to account for this presumable complexity of networks involved in emotion regulation. This was accomplished by spatial decomposition of BOLD activation patterns of the baseline resting-state into 20 spatial networks. Statistical comparisons to recently and robustly reported resting-state networks (RSN) (Damoiseaux et al., 2006; Smith et al., 2009, 2014) confirmed their validity. Mapping them into each individual subject's space each for resting-session 1 and 2 and consecutively performing group comparisons with dual regression disclosed that none of the 20 RSNs was differentially affected by picture emotionality.

Remarkably, complementing evidence for this apparent non-susceptibility towards emotional pictures in amygdala-FC and RSNs in the time following immediate emotion processing was given by our finding that the fractional amplitude of low frequency fluctuations (fALFF) in the amygdala showed no relation to picture valence.

As opposed to the neurofunctional data, behavioral measures were differentially affected by picture valence. Compared to neutral pictures, negative pictures were rated as more negative and arousing, and were remembered better. Since the recall of geometrical figures was independent of picture emotionality, this memory-facilitating effect was not ascribable to general memory performance. Research designed to look into memory consolidation has revealed that rs-FC directly after encoding may be predictive both of later recall performance of visual stimuli, e.g. associations between post-encoding rs-FC of the hippocampus and memory performance about 60 min afterwards (Tambini et al., 2010), and of links between inter-network-FC and memory performance 6.5 weeks later (Sneve et al., 2017). In the current experimental paradigm, which is not primarily aimed at investigating memory dynamics, we found no valence-dependent effects on hippocampus-whole brain-FC. However, for hippocampus-FC to be related to later memory performance, time window may be particularly important. In line with this, rs-FC between the parietal memory network and DMN after encoding

correlates with memory capacity when tested 6.5 weeks but not 1.5 h later (Sneve et al., 2017). These findings indicate that rs-FC is hardly susceptible to preceding processing of visual emotional stimuli.

Fluctuations in vigilance (Olbrich et al., 2009) and different sleep stages (Tagliazucchi et al., 2012) may co-vary with changes in rs-FC. There was a report of a reliable loss of wakefulness within 3 min rs-fMRI in one third of subjects, grounded on an analysis of 1147 datasets (Tagliazucchi and Laufs, 2014). Notably, in the current study, out of 31 and 32 subjects during resting-session 1 and 2, respectively, for whom we had valid EEG data, the large majority of subjects was in a state of relaxed wakefulness at most time points (summarized over 3 s). The binary first-level regressor vigilance had no impact on the BOLD signal. It is thus unlikely that vigilance, a physiological state defined according to previously adapted concepts (Hegerl et al., 2008; Olbrich et al., 2009), operated as a confounder in this study. Owing to the risk of oversimplification of the dynamic and gradual process of sleep onset (Prerau et al., 2014) and due to subjective reports of wakefulness from our subjects, we refrained from a discrete categorization of wake/sleep.

Prolonged activation in amygdala-FC networks following acute stressors has been reported, an effect suggested to constitute an extended state of hypervigilance (Clewett et al., 2013; van Marle et al., 2010; Veer et al., 2011). In accordance with this stress perspective, stress-induced neuroendocrine levels may regulate amygdala-FC in the recovery phase from acute stressors (Quaedflieg et al., 2015), and acute painful stressors alter amygdala-FC with frontal and anterior cingular cortex (ACC) regions 15 to 30 min after stressor onset (Clewett et al., 2013). This framework differs from ours in that we did not apply acute stressors (e.g., psychological stress test, painful interventions). Even if a substantial increase in corticosteroids were elicited by the emotion induction peak levels could be expected only after 30 min. Yet, one study reported enhanced amygdala-FC with the dorsal ACC, AI, and LC after viewing a 1.5 min highly aversive movie clip (van Marle et al., 2010). In contrast to our study design, the movie clip might have induced a stressful state reflected in lasting changes in rs-FC. Moreover, they conducted the rs-fMRI without time delay after cessation of the movie, which was presented inside the scanner. Importantly, the stress induction paradigms used in these studies substantially differ from our emotion induction paradigm.

The present study has several limitations: Due to the setting of the pictorial rating task at the computer outside the scanner, we could not measure BOLD-related brain activity during the pictorial rating task. Although EEG data during this task was available, it could not be properly analyzed due to major movement-related artifacts. Yet, a multitude of studies has demonstrated the amygdala to be activated upon viewing negative pictures (Banks et al., 2007; Eippert et al., 2007; Erk et al., 2010; Fastenrath et al., 2014; Radua et al., 2014; Townsend et al., 2013; Walter et al., 2009). Moreover, the memory-facilitating effect of picture emotionality also found in our study is known to rely on the amygdala's initial involvement (e.g., Fastenrath et al., 2014; Kim, 2011; McGaugh, 2004). Nonetheless, future studies should include brain activation measures also during the emotion induction task. Furthermore, we cannot generalize to other emotional tasks. It may well be that stronger and more ecologically valid emotion induction paradigms (Schilbach, 2016; Xie et al., 2016) might have induced alterations in the resting-state measures applied in the present study. A further limitation is the number of subjects ($N = 34$), which may be regarded relatively small given the unconstrained nature of the resting-state (Finn et al., 2017). Therefore, the negative results should be treated with caution and tested for replication in larger samples.

The progress towards incorporation of rs-FC measures as clinical biomarkers (Camchong et al., 2013; Drysdale et al., 2017; Gong et al., 2014; Sorg et al., 2013; Verduyn et al., 2015; Whitfield-Gabrieli et al., 2016; Wilcox et al., 2016; Yang et al., 2014; Zotev et al., 2013) will require minimization of confounding factors to allow for a standardized setting. Concerning this, it is essential to unveil factors affecting rs-FC. Factors eliciting emotional responses in everyday life, like negative emotional stimuli and daily hassles, may be hard to control for by clinicians. In this line of thoughts, we believe our findings provide important insight into the requirements for measurement standardization, a key challenge for rs-fMRI. Yet, rs-fMRI-specific confounds may vary with mental health status, which is particularly important given the planned implication of rs-fMRI in patients with tentative diagnoses. The pathological correlates of mental disorders that have been associated with traumatic experiences, such as post-traumatic stress disorder (PTSD) and borderline personality disorder (Bandelow et al., 2005; Golier et al., 2003), have been proposed to be escalates of brain activation patterns observed in the healthy confronted with ethically acceptable aversive emotional stimuli. PTSD, as an example, may be regarded as a disorder of recovery from the early responses to traumatic events (Shalev, 2009). In cases of pathological anxiety, excessive apprehension occurs upon minimally threatening stimuli, implying dysfunction at the level of interpretation (Calhoon and Tye, 2015). It is important to understand what factors exacerbate or protect against disadvantageous reactions to emotional stimuli. Amygdala-FC may form a critical juncture for affective reactivity, culminating in individual patterns of immediate emotion processing and emotion regulation. Future studies may want to investigate those transient states of emotion regulation in clinical samples.

Conclusions

In summary, our findings demonstrate that several resting-state measures, which had been hypothesized to be involved in the temporal dynamics of emotion processing following exposure to emotional pictorial stimuli, transpired unaffected by such an intervention. Future research should include additional emotion induction paradigms and might investigate if resting-state functional connectivity in patients with problems in emotion regulation, as it is commonly observed in depression or anxiety disorders, might be more susceptible to emotion induction.

Acknowledgements and funding source declaration

This project has mainly been sponsored by Bilddiagnostik.ch, directed at the time by Alfred Geissmann, who generously provided the MRI materials and personnel assistance, by the MCN, University of Basel, head of which is Prof. de Quervain, in providing personnel and the funds for participant reimbursement, and the UPK Basel, in providing EEG materials and professional support. Our gratitude also goes particularly to Amanda Aerni and Franck Girard.

Appendix A. Supplementary data

Supplementary data related to this article can be found at https://doi.org/10.1016/j.neuroimage.2017.11.046.

Legal statements

All authors certify that this work has been submitted in accordance with their agreement. They warrant that the article is the authors' original work and has not been published previously. Part of this work has been presented in a poster on the Fifth Biennial Conference of Resting State and Brain

Connectivity (2016) in Vienna, Austria, by the first author (L.G.). The authors further declare that there are no conflicts of interest. The study has been conducted in accordance with the Declaration of Helsinki.

References

Allen, P.J., Josephs, O., Turner, R., 2000. A method for removing imaging artifact from continuous EEG recorded during functional MRI. NeuroImage 12 (2), 230–239. http://doi.org/10.1006/nimg.2000.0599.

Andrews-Hanna, J.R., Snyder, A.Z., Vincent, J.L., Lustig, C., Head, D., Raichle, M.E., Buckner, R.L., 2007. Disruption of large-scale brain systems in advanced aging. Neuron 56 (5), 924–935. http://doi.org/10.1016/j.neuron.2007.10.038.

Ashburner, J., 2007. A fast diffeomorphic image registration algorithm. NeuroImage 38 (1), 95–113. http://doi.org/10.1016/j.neuroimage.2007.07.007.

Bandelow, B., Krause, J., Wedekind, D., Broocks, A., Hajak, G., Rüther, E., 2005. Early traumatic life events, parental attitudes, family history, and birth risk factors in patients with borderline personality disorder and healthy controls. Psychiatry Res. 134 (2), 169–179. http://doi.org/10.1016/j.psychres.2003.07.008.

Banks, S.J., Eddy, K.T., Angstadt, M., Nathan, P.J., Luan Phan, K., 2007. Amygdala-frontal connectivity during emotion regulation. Soc. Cognitive Affect. Neurosci. 2 (4), 303–312. http://doi.org/10.1093/scan/nsm029.

Barkhof, F., Haller, S., Rombouts, S.A.R.B., 2014. Resting-state functional MR imaging: a new window to the brain. Radiology 272 (1), 29–49. http://doi.org/10.1148/radiol.14132388.

Baumann, O., Mattingley, J.B., 2012. Functional topography of primary emotion processing in the human cerebellum. NeuroImage 61 (4), 805–811. http://doi.org/10.1016/j.neuroimage.2012.03.044.

Behzadi, Y., Restom, K., Liau, J., Liu, T.T., 2007. A component based noise correction method (CompCor) for BOLD and perfusion based fMRI. NeuroImage 37 (1), 90–101. http://doi.org/10.1016/j.neuroimage.2007.04.042.

Biswal, B., Mennes, M., Zuo, X.-N., Gohel, S., Kelly, C., Smith, S.M., Milham, M.P., 2010. Toward discovery science of human brain function. Proc. Natl. Acad. Sci. U. S. A. 107 (10), 4734–4739. http://doi.org/10.1073/pnas.0911855107.

Borkenau, P., Ostendorf, F., 1993. NEO-Fünf-Faktoren-Inventar (NEO-FFI) nach Costa und McCrae. Handanweisung. Hogrefe, Göttingen.

Calhoon, G.G., Tye, K.M., 2015. Resolving the neural circuits of anxiety. Nat. Neurosci. 18 (10), 1394–1404. http://doi.org/10.1038/nn.4101.

Camchong, J., Stenger, A., Fein, G., 2013. Resting-state synchrony during early alcohol abstinence can predict subsequent relapse. Cereb. Cortex 23 (9), 2086–2099. http://doi.org/10.1093/cercor/bhs190.

Chai, X.J., Ofen, N., Gabrieli, J.D.E., Whitfield-Gabrieli, S., 2014. Development of deactivation of the default-mode network during episodic memory formation. NeuroImage 84, 932–938. http://doi.org/10.1016/j.neuroimage.2013.09.032.

Chai, X.J., Whitfield-Gabrieli, S., Shinn, A.K., Nieto-Castanon, A., Mccarthy, J.M., Cohen, B.M., 2011. Abnormal medial prefrontal cortex resting-state connectivity in bipolar disorder and schizophrenia. Neuropsychopharmacology 36, 2009–2017. http://doi.org/10.1038/npp.2011.88.

Chao-Gan, Y., Yu-Feng, Z., 2010. DPARSF: a MATLAB toolbox for "pipeline" data analysis of resting-state fMRI. Front. Syst. Neurosci. 4 (13). http://doi.org/10.3389/fnsys.2010.00013.

Clewett, D., Schoeke, A., Mather, M., 2013. Amygdala functional connectivity is reduced after the cold pressor task. Cognitive, Affect. Behav. Neurosci. 13 (3), 501–518. http://doi.org/10.3758/s13415-013-0162-x.

Damoiseaux, J.S., Rombouts, S.A.R.B., Barkhof, F., Scheltens, P., Stam, C.J., Smith, S.M., Beckmann, C.F., 2006. Consistent resting-state networks across healthy subjects. Proc. Natl. Acad. Sci. U. S. A. 103 (37), 13848–13853.

Drysdale, A.T., Grosenick, L., Downar, J., Dunlop, K., Mansouri, F., Meng, Y., Liston, C., 2017. Resting-state connectivity biomarkers define neurophysiological subtypes of depression. Nat. Med. 23 (1), 28–38. http://doi.org/10.1038/nm.4246.

Eippert, F., Veit, R., Weiskopf, N., Erb, M., Birbaumer, N., Anders, S., 2007. Regulation of emotional responses elicited by threat-related stimuli. Hum. Brain Mapp. 28 (5), 409–423. http://doi.org/10.1002/hbm.20291.

Erk, S., Mikschl, A., Stier, S., Ciaramidaro, A., Gapp, V., Weber, B., Walter, H., 2010. Acute and sustained effects of cognitive emotion regulation in major depression. J. Neurosci. 30 (47), 15726–15734. http://doi.org/10.1523/JNEUROSCI.1856-10.2010.

Fair, D., Cohen, A.L., Dosenbach, N.U.F., Church, J.A., Miezin, F.M., Barch, D.M., Schlaggar, B.L., 2008. The maturing architecture of the brain's default network. Proc. Natl. Acad. Sci. U. S. A. 105 (10), 4028–4032. http://doi.org/10.1073/pnas.0800376105.

Fastenrath, M., Coynel, D., Spalek, K., Milnik, A., Gschwind, L., Roozendaal, B., de Quervain, D.J.F., 2014. Dynamic modulation of amygdala-hippocampal connectivity by emotional arousal. J. Neurosci. 34 (42), 13935–13947. http://doi.org/10.1523/JNEUROSCI.0786-14.2014.

Ferreira, L.K., Busatto, G.F., 2013. Resting-state functional connectivity in normal brain aging. Neurosci. Biobehav. Rev. 37 (3), 384–400. http://doi.org/10.1016/j.neubiorev.2013.01.017.

Filippini, N., Macintosh, B.J., Hough, M.G., Goodwin, G.M., Frisoni, G.B., Smith, S.M., Mackay, C.E., 2009. Distinct patterns of brain activity in young carriers of the APOE-4 allele. Proc. Natl. Acad. Sci. U. S. A. 106 (17), 7209–7214. http://doi.org/10.1073/pnas.0811879106.

Finn, E.S., Scheinost, D., Finn, D.M., Shen, X., Papademetris, X., Constable, R.T., 2017. Can brain state be manipulated to emphasize individual differences in functional connectivity? NeuroImage 160, 140–151 (Advance online publication). http://doi.org/10.1016/j.neuroimage.2017.03.064.

Fischl, B., Salat, D.H., Busa, E., Albert, M., Dieterich, M., Haselgrove, C., Dale, A.M., 2002. Whole brain segmentation: automated labeling of neuroanatomical structures in the human brain. Neuron 33 (3), 341–355. http://doi.org/10.1016/S0896-6273(02)00569-X.

Friston, K.J., Williams, S., Howard, R., Frackowiak, R.S., Turner, R., 1996. Movement-related effects in fMRI time-series. Magnetic Reson. Med. 35 (3), 346–355. http://doi.org/10.1002/mrm.1910350312.

Ghashghaei, H.T., Barbas, H., 2002. Pathways for emotion: interactions of prefrontal and anterior temporal pathways in the amygdala of the rhesus monkey. Neuroscience 115 (4), 1261–1279. http://doi.org/10.1016/S0306-4522(02)00446-3.

Golier, J. a, Yehuda, R., Bierer, L.M., Mitropoulou, V., New, A.S., Schmeidler, J., Siever, L.J., 2003. The relationship of borderline personality disorder to posttraumatic stress disorder and traumatic events. Am. J. Psychiatry 160 (11), 2018–2024. http://doi.org/10.1176/appi.ajp.160.11.2018.

Gong, Q., Li, L., Du, M., Pettersson-Yeo, W., Crossley, N., Yang, X., Mechelli, A., 2014. Quantitative prediction of individual psychopathology in trauma survivors using resting-state fMRI. Neuropsychopharmacology 39 (3), 681–687. http://doi.org/10.1038/npp.2013.251.

Hautzinger, M., Bailer, M., 1993. Allgemeine Depressionsskala. Beltz Verlag, Weinheim.

Heck, A., Fastenrath, M., Ackermann, S., Auschra, B., Bickel, H., Coynel, D., Papassotiropoulos, A., 2014. Converging genetic and functional brain imaging evidence links neuronal excitability to working memory, psychiatric disease, and brain activity. Neuron 81 (5), 1203–1213. http://doi.org/10.1016/j.neuron.2014.01.010.

Hegerl, U., Stein, M., Mulert, C., Mergl, R., Olbrich, S., Dichgans, E., Pogarell, O., 2008. EEG-vigilance differences between patients with borderline personality disorder, patients with obsessive-compulsive disorder and healthy controls. Eur. Archives Psychiatry Clin. Neurosci. 258 (3), 137–143. http://doi.org/10.1007/s00406-007-0765-8.

Hjelmervik, H., Hausmann, M., Osnes, B., Westerhausen, R., Specht, K., 2014. Resting states are resting traits - an fMRI study of sex differences and menstrual cycle effects in resting state cognitive control networks. PLoS One 9 (7), 32–36. http://doi.org/10.1371/journal.pone.0103492.

Höistad, M., Barbas, H., 2008. Sequence of information processing for emotions through pathways linking temporal and insular cortices with the amygdala. NeuroImage 40 (3), 1016–1033. http://doi.org/10.1016/j.neuroimage.2007.12.043.

Iannetti, G.D., Niazy, R.K., Wise, R.G., Jezzard, P., Brooks, J.C.W., Zambreanu, L., Tracey, I., 2005. Simultaneous recording of laser-evoked brain potentials and continuous, high-field functional magnetic resonance imaging in humans. NeuroImage 28 (3), 708–719. http://doi.org/10.1016/j.neuroimage.2005.06.060.

Jenkinson, M., Beckmann, C.F., Behrens, T.E.J., Woolrich, M.W., Smith, S.M., 2012. FSL. NeuroImage 62 (2), 782–790. http://doi.org/10.1016/j.neuroimage.2011.09.015.

Johns, M.W., 1991. A new method for measuring daytime sleepiness: the Epworth sleepiness scale. Sleep 14 (6), 540–545.

Kerr, K.L., Avery, J.A., Barcalow, J.C., Moseman, S.E., Bodurka, J., Bellgowan, P.S.F., Simmons, W.K., 2015. Trait impulsivity is related to ventral ACC and amygdala activity during primary reward anticipation. Soc. Cognitive Affect. Neurosci. 10 (1), 36–42. http://doi.org/10.1093/scan/nsu023.

Kim, H., 2011. Neural activity that predicts subsequent memory and forgetting: a meta-analysis of 74 fMRI studies. NeuroImage 54 (3), 2446–2461. http://doi.org/10.1016/j.neuroimage.2010.09.045.

Kim, M.J., Loucks, R. a, Palmer, A.L., Brown, A.C., Solomon, K.M., Marchante, A.N., Whalen, P.J., 2011. The structural and functional connectivity of the amygdala: from normal emotion to pathological anxiety. Behav. Brain Res. 223 (2), 403–410. http://doi.org/10.1016/j.bbr.2011.04.025.

Laird, A.R., Fox, M.P., Eickhoff, S.B., Turner, J.A., Ray, K.L., McKay, D.R., Fox, P.T., 2011. Behavioral interpretations of intrinsic connectivity networks. J. Cognitive Neurosci. 23 (12), 4022–4037. http://doi.org/10.1162/jocn_a_00077.

Lang, P.J., Bradley, M.M., Cuthbert, B.N., 2005. International Affective Picture System (IAPS): Affective Ratings of Pictures and Instruction Manual (Technical). University of Florida, Gainesville, FL.

Larsen, R.J., Diener, E., 1987. Affect intensity as an individual difference characteristic: a review. J. Res. Personality 21 (1), 1–39. http://doi.org/10.1016/0092-6566(87)90023-7.

Laux, L., Glanzmann, P., Schaffner, P., Spielberger, C.D., 1981. Das State-Trait-Angstinventar. Theoretische Grundlagen und Handanweisung. Beltz Test GmbH, Weinheim.

Manning, J., Reynolds, G., Saygin, Z.M., Hofmann, S.G., Pollack, M., Gabrieli, J.D.E., Whitfield-Gabrieli, S., 2015. Altered resting-state functional connectivity of the frontal-striatal reward system in social anxiety disorder. PLoS One 10 (4), e0125286. http://doi.org/10.1371/journal.pone.0125286.

McGaugh, J.L., 2004. The amygdala modulates the consolidation of memories of emotionally arousing experiences. Annu. Rev. Neurosci. 27, 1–28. http://doi.org/10.1146/annurev.neuro.27.070203.144157.

Moosmann, M., Schönfelder, V.H., Specht, K., Scheeringa, R., Nordby, H., Hugdahl, K., 2009. Realignment parameter-informed artefact correction for simultaneous EEG-fMRI recordings. NeuroImage 45 (4), 1144–1150. http://doi.org/10.1016/j.neuroimage.2009.01.024.

Morey, R.A., Petty, C.M., Xu, Y., Hayes, J.P., Wagner, H.R., Lewis, D.V., McCarthy, G., 2009. A comparison of automated segmentation and manual tracing for quantifying hippocampal and amygdala volumes. NeuroImage 45 (3), 855–866. http://doi.org/10.1016/j.neuroimage.2008.12.033.

Murty, V.P., Ritchey, M., Adcock, R.A., LaBar, K.S., 2010. fMRI studies of successful emotional memory encoding: a quantitative meta-analysis. Neuropsychologia 48 (12), 3459–3469. http://doi.org/10.1016/j.neuropsychologia.2010.07.030.

Niazy, R.K., Beckmann, C.F., Iannetti, G.D., Brady, J.M., Smith, S.M., 2005. Removal of FMRI environment artifacts from EEG data using optimal basis sets. NeuroImage 28 (3), 720–737. http://doi.org/10.1016/j.neuroimage.2005.06.067.

Olbrich, S., Mulert, C., Karch, S., Trenner, M., Leicht, G., Pogarell, O., Hegerl, U., 2009. EEG-vigilance and BOLD effect during simultaneous EEG/fMRI measurement. NeuroImage 45 (2), 319–332. http://doi.org/10.1016/j.neuroimage.2008.11.014.

Oldfield, R.C., 1971. The assessment and analysis of handedness: the Edinburgh inventory. Neuropsychologia 9 (1), 97–113.

Passamonti, L., Rowe, J.B., Ewbank, M., Hampshire, A., Keane, J., Calder, A.J., 2008. Connectivity from the ventral anterior cingulate to the amygdala is modulated by appetitive motivation in response to facial signals of aggression. NeuroImage 43 (3), 562–570. http://doi.org/10.1016/j.neuroimage.2008.07.045.

Patenaude, B., Smith, S.M., Kennedy, D.N., Jenkinson, M., 2011. A Bayesian model of shape and appearance for subcortical brain segmentation. NeuroImage 56 (3), 907–922. http://doi.org/10.1016/j.neuroimage.2011.02.046.

Phan, K.L., Wager, T., Taylor, S.F., Liberzon, I., 2002. Functional neuroanatomy of emotion: a meta-analysis of emotion activation studies in PET and fMRI. NeuroImage 16 (2), 331–348. http://doi.org/10.1006/nimg.2002.1087.

Phelps, E.A., LeDoux, J.E., 2005. Contributions of the amygdala to emotion processing: from animal models to human behavior. Neuron 48 (2), 175–187. http://doi.org/10.1016/j.neuron.2005.09.025.

Prerau, M.J., Hartnack, K.E., Obregon-Henao, G., Sampson, A., Merlino, M., Gannon, K., Purdon, P.L., 2014. Tracking the sleep onset process: an empirical model of behavioral and physiological dynamics. PLoS Comput. Biol. 10 (10), e1003866. http://doi.org/10.1371/journal.pcbi.1003866.

Quaedflieg, C.W.E.M., Van De Ven, V., Meyer, T., Siep, N., Merckelbach, H., Smeets, T., 2015. Temporal dynamics of stress-induced alternations of intrinsic amygdala connectivity and neuroendocrine levels. PLoS One 10 (5), e0124141. http://doi.org/10.1371/journal.pone.0124141.

R Core Team, 2015. R: a language and environment for statistical computing. R Found. Stat. Comput. Retrieved from http://www.r-project.org/.

Radua, J., Sarró, S., Vigo, T., Alonso-Lana, S., Bonnín, C.M., Ortiz-Gil, J., Pomarol-Clotet, E., 2014. Common and specific brain responses to scenic emotional stimuli. Brain Struct. Funct. 219 (4), 1463–1472. http://doi.org/10.1007/s00429-013-0580-0.

Rasch, B., Spalek, K., Buholzer, S., Luechinger, R., Boesiger, P., Papassotiropoulos, A., de Quervain, D.J.-F., 2009. A genetic variation of the noradrenergic system is related to differential amygdala activation during encoding of emotional memories. Proc. Natl. Acad. Sci. U. S. A. 106 (45), 19191–19196. http://doi.org/10.1073/pnas.0907425106.

Rechtschaffen, A., Kales, A., 1968. A Manual of Standardized Terminology, Techniques and Scoring System for Sleep Stages of Human Subjects. University of California, Los Angeles.

Richardson, M.P., Strange, B.A., Dolan, R.J., 2004. Encoding of emotional memories depends on amygdala and hippocampus and their interactions. Nat. Neurosci. 7 (3), 278–285. http://doi.org/10.1038/nn1190.

Riedel, M.C., Ray, K.L., Dick, A.S., Sutherland, M.T., Hernandez, Z., Fox, P.M., Laird, A.R., 2015. Meta-analytic connectivity and behavioral parcellation of the human cerebellum. NeuroImage 117, 327–342. http://doi.org/10.1016/j.neuroimage.2015.05.008.

Roozendaal, B., McEwen, B.S., Chattarji, S., 2009. Stress, memory and the amygdala. Nat. Rev. Neurosci. 10 (6), 423–433. http://doi.org/10.1038/nrn2651.

Roy, A.K., Shehzad, Z., Margulies, D.S., Kelly, a.M. C., Uddin, L.Q., Gotimer, K., Milham, M.P., 2009. Functional connectivity of the human amygdala using resting state fMRI. NeuroImage 45 (2), 614–626. http://doi.org/10.1016/j.neuroimage.2008.11.030.

Schilbach, L., 2016. Towards a second-person neuropsychiatry. Philosophical Trans. R. Soc. B Biol. Sci. 371 (1686). http://doi.org/10.1098/rstb.2015.0081.

Shalev, A.Y., 2009. Posttraumatic stress disorder (PTSD) and stress related disorders. Psychiatric Clin. N. Am. 32 (3), 687–704. http://doi.org/10.1016/j.psc.2009.06.001.

Sheline, Y.I., Price, J.L., Yan, Z., Mintun, M.A., 2010. Resting-state functional MRI in depression unmasks increased connectivity between networks via the dorsal nexus. Proc. Natl. Acad. Sci. U. S. A. 107 (24), 11020–11025. http://doi.org/10.1073/pnas.1000446107.

Smith, S.M., Fox, P.T., Miller, K.L., Glahn, D.C., Fox, P.M., Mackay, C.E., Beckmann, C.F., 2009. Correspondence of the brain's functional architecture during activation and rest. Proc. Natl. Acad. Sci. U. S. A. 106 (31), 13040–13045. http://doi.org/10.1073/pnas.0905267106.

Smith, D.V., Utevsky, A.V., Bland, A.R., Clement, N., Clithero, J. a., Harsch, A.E.W., Huettel, S. a, 2014. Characterizing individual differences in functional connectivity using dual-regression and seed-based approaches. NeuroImage 95, 1–12. http://doi.org/10.1016/j.neuroimage.2014.03.042.

Sneve, M.H., Grydeland, H., Amlien, I.K., Langnes, E., Walhovd, K.B., Fjell, A.M., 2017. Decoupling of large-scale brain networks supports the consolidation of durable episodic memories. NeuroImage 153, 336–345. http://doi.org/10.1016/j.neuroimage.2016.05.048.

Sorg, C., Manoliu, A., Neufang, S., Myers, N., Peters, H., Schwerthöffer, D., Riedl, V., 2013. Increased intrinsic brain activity in the striatum reflects symptom dimensions in schizophrenia. Schizophr. Bull. 39 (2), 387–395. http://doi.org/10.1093/schbul/sbr184.

Spreen, O., Strauss, E., 1991. A Compendium of Neuropsychological Tests: Administration, Norms and Commentary. Oxford University Press, New York, Oxford.

Tagliazucchi, E., Laufs, H., 2014. Decoding wakefulness levels from typical fMRI resting-state data reveals reliable drifts between wakefulness and sleep. Neuron 82 (3), 695–708. http://doi.org/10.1016/j.neuron.2014.03.020.

Tagliazucchi, E., von Wegner, F., Morzelewski, A., Borisov, S., Jahnke, K., Laufs, H., 2012. Automatic sleep staging using fMRI functional connectivity data. NeuroImage 63 (1), 63–72. http://doi.org/10.1016/j.neuroimage.2012.06.036.

Tambini, A., Ketz, N., Davachi, L., 2010. Enhanced brain correlations during rest are related to memory for recent experiences. Neuron 65 (2), 280–290. http://doi.org/10.1016/j.neuron.2010.01.001.

Townsend, J.D., Torrisi, S.J., Lieberman, M.D., Sugar, C.A., Bookheimer, S.Y., Altshuler, L.L., 2013. Frontal-amygdala connectivity alterations during emotion downregulation in bipolar I disorder. Biol. Psychiatry 73 (2), 127–135. http://doi.org/10.1016/j.biopsych.2012.06.030.

van den Heuvel, M.P., Hulshoff Pol, H.E., 2010. Exploring the brain network: a review on resting-state fMRI functional connectivity. Eur. Neuropsychopharmacol. 20 (8), 519–534. http://doi.org/10.1016/j.euroneuro.2010.03.008.

van Marle, H.J.F., Hermans, E.J., Qin, S., Fernández, G., 2010. Enhanced resting-state connectivity of amygdala in the immediate aftermath of acute psychological stress. NeuroImage 53 (1), 348–354. http://doi.org/10.1016/j.neuroimage.2010.05.070.

Veer, I.M., Oei, N.Y.L., Spinhoven, P., van Buchem, M.A., Elzinga, B.M., Rombouts, S.A.R.B., 2011. Beyond acute social stress: increased functional connectivity between amygdala and cortical midline structures. NeuroImage 57 (4), 1534–1541. http://doi.org/10.1016/j.neuroimage.2011.05.074.

Venkatraman, A., Edlow, B.L., Immordino-Yang, M.H., 2017. The brainstem in emotion: a review. Front. Neuroanat. 11, 1–12. http://doi.org/10.3389/fnana.2017.00015.

Verduyn, P., Delaveau, P., Rotge, J.-Y., Fossati, P., Van Mechelen, I., 2015. Determinants of emotion duration and underlying psychological and neural mechanisms. Emot. Rev. 7 (4), 330–335. http://doi.org/10.1177/1754073915590618.

Walter, H., von Kalckreuth, A., Schardt, D., Stephan, A., Goschke, T., Erk, S., 2009. The temporal dynamics of voluntary emotion regulation. PLoS One 4 (8), e6726. http://doi.org/10.1371/journal.pone.0006726.

Waugh, C.E., Schirillo, J. a, 2012. Timing: a missing key ingredient in typical fMRI studies of emotion. Behav. Brain Sci. 35 (3), 170–171. http://doi.org/10.1017/S0140525X11001646.

Whitfield-Gabrieli, S., Ghosh, S.S., Nieto-Castanon, A., Saygin, Z., Doehrmann, O., Chai, X.J., Gabrieli, J.D., 2016. Brain connectomics predict response to treatment in social anxiety disorder. Mol. Psychiatry 21 (5), 680–685. http://doi.org/10.1038/mp.2015.109.

Whitfield-Gabrieli, S., Nieto-Castanon, A., 2012. Conn: a functional connectivity toolbox for correlated and anticorrelated brain networks. Brain Connect. 2 (3), 125–141. http://doi.org/10.1089/brain.2012.0073.

Wilcox, C.E., Pommy, J.M., Adinoff, B., 2016. Neural circuitry of impaired emotion regulation in substance use disorders. Am. J. Psychiatry 173 (4), 344–361. http://doi.org/10.1176/appi.ajp.2015.15060710.

Winkler, A.M., Ridgway, G.R., Webster, M.A., Smith, S.M., Nichols, T.E., 2014. Permutation inference for the general linear model. NeuroImage 92, 381–397. http://doi.org/10.1016/j.neuroimage.2014.01.060.

Xie, C., Li, S.J., Shao, Y., Fu, L., Goveas, J., Ye, E., Yang, Z., 2011. Identification of hyperactive intrinsic amygdala network connectivity associated with impulsivity in abstinent heroin addicts. Behav. Brain Res. 216 (2), 639–646. http://doi.org/10.1016/j.bbr.2010.09.004.

Xie, X., Bratec, S.M., Schmid, G., Meng, C., Doll, A., Wohlschläger, A., Sorg, C., 2016. How do you make me feel better? Social cognitive emotion regulation and the default mode network. NeuroImage 134, 270–280. http://doi.org//10.1016/j.neuroimage.2016.04.015.

Yang, Z., Xu, Y., Xu, T., Hoy, C.W., Handwerker, D.A., Chen, G., Bandettini, P.A., 2014. Brain network informed subject community detection in early-onset schizophrenia. Sci. Rep. 4, 5549. http://doi.org/10.1038/srep05549.

Zotev, V., Phillips, R., Young, K.D., Drevets, W.C., Bodurka, J., 2013. Prefrontal control of the amygdala during real-time fMRI neurofeedback training of emotion regulation. PLoS One 8 (11), e79184. http://doi.org/10.1371/journal.pone.0079184.

Zotev, V., Phillips, R., Yuan, H., Misaki, M., Bodurka, J., 2014. Self-regulation of human brain activity using simultaneous real-time fMRI and EEG neurofeedback. NeuroImage 85 (3), 985–995. http://doi.org/10.1016/j.neuroimage.2013.04.126.

Zou, Q.H., Zhu, C.Z., Yang, Y., Zuo, X.N., Long, X.Y., Cao, Q.J., Zang, Y.F., 2008. An improved approach to detection of amplitude of low-frequency fluctuation (ALFF) for resting-state fMRI: fractional ALFF. J. Neurosci. Methods 172 (1), 137–141. http://doi.org/10.1016/j.jneumeth.2008.04.012.